Decolorization of Direct Black 22 by Photo Fenton like Method Using UV Light and Zeolite Modified Zinc Ferrite: Kinetics and Thermodynamics

4 Serap FINDIK^{1,*}

¹Hitit University, Engineering Faculty, Chemical Engineering Department, Kuzey Yerleskesi, Çevre Yolu Bulvarı, 19030, Çorum, Türkiye

*Corresponding author: E-mail: serapfindik@hitit.edu.tr

Abstract

In this study, a heterogeneous catalyst was prepared to enhance photo-Fenton like oxidation of Direct Black-22 (DB-22). Zeolite modified with zinc ferrite was used as a catalyst. The prepared catalyst was characterized using FTIR, SEM, EDS and XRD. The effect of various parameters like catalyst modification with HCl, H₂O₂ amount, catalyst amount, CaCl₂ amount, initial pH, initial concentration and temperature on the decolorization of DB-22 was studied under UV light. Kinetic and thermodynamic properties were investigated. The highest decolorization of DB-22 was found to be 93.3% under the following conditions: initial concentration: 0.070 g/L, initial temperature: 25 °C, original pH, H₂O₂ amount: 2.78 g/L, m-ZZF amount: 3 g/L, CaCl₂ amount: 3.75 g/L, reaction time: 60 min and UV light. The activation energy was found to be -14.76 kJ/mol under the studied conditions. The decolorization reaction was an exothermic reaction, and the calculated reaction enthalpy was -17.31 kJ/mol. The activation entropy was calculated to be -0.326 kJ/mol. The standard Gibbs free energy change of the activation had a positive value, and it increased with increasing temperature.

1. Introduction

Keywords: Direct black 22, photo-Fenton process, UV, zeolite, zinc ferrite

Textile dyes account for more than half of the total dye production in the world. The dyes used in the dyeing process cause the formation of textile wastewater. This wastewater causes coloration in natural water resources, as well as damaging living organisms and preventing the passage of sunlight. In addition, when mixed with drinking water, it harms human life due to its carcinogenic nature. Removing these dyes from water is important to prevent environmental damage.¹

Conventional treatment methods such as biological treatment, coagulation, adsorption, chemical precipitation, solvent extraction, filtration, and electrochemical treatment are ineffective for decolorization of dyes.^{2,3} They also have some disadvantages such as incomplete destruction of dye,

high energy consumption, high operating cost, poor selectivity, incomplete ion removal, and generation of toxic sludge and waste product. Advanced oxidation methods are preferred for dye removal because of their simplicity and effectiveness. Advanced oxidation methods are based on the production of the OH• radicals. The homogeneous Fenton process is a Fenton reaction in which iron salts are used as catalysts. In this process, hydrogen peroxide, which is used as an oxidant, and iron ions, which are used as a catalyst, react to produce OH• radicals. The use of H₂O₂ and Fenton reagents with UV light has been known as photo-Fenton oxidation system. UV light irradiation and Fenton reagents cause an increase in the OH• formation rate. Additional OH• radicals are formed by either photoreduction of ferric ions (Fe³⁺) to ferrous ions (Fe²⁺) or hydrogen peroxide photolysis. 2,3,6

Fenton oxidation systems based on the homogeneous Fenton reagent ($Fe^{2+}/Fe^{3+}/H_2O_2$) have some disadvantages such as narrow pH range, removal of sludge containing iron ions, and requirement of large amount of chemicals. Therefore, heterogeneous Fenton reactions are preferred to eliminate the negative effects of homogeneous Fenton reactions.

In the heterogeneous catalyst, the iron is stabilized into the catalyst interlayer space. Hydroxyl radicals are produced by oxidation of hydrogen peroxide with neither pH control nor precipitation of iron hydroxide.⁶

In heterogeneous Fenton-like processes, spinel ferrites (MFe₂O₄) can be used as a heterogeneous catalyst. The term M in spinel ferrite structure refers to the divalent metal ions such as Ni²⁺, Mn²⁺, Co²⁺, Mg²⁺, Cu²⁺, Zn²⁺ etc. Spinel ferrites such as ZnFe₂O₄, CoFe₂O₄, and NiFe₂O₄ are used in medicines, sensors, and catalyst carriers thanks to their high mechanical strength, magnetic properties, unique structure, and catalytic performance.^{7,8}

The use of zeolites modified with semiconductors can be an alternative catalyst for a variety of important reactions. ^{1,2} Zeolites are crystalline aluminosilicates with cavities, unique structures and chemical compositions, uniform pores and channels, high surface area, thermal stability, and an excellent adsorption ability. Conventional zeolites are constructed by tetrahedral SiO₄ and AlO₄ units. ^{1,9,10} There are at least 41 known types of natural zeolite. ¹ Some of the most known and abundant types of natural zeolite are clinoptilolite, phillipsite, heulandite, mordenite, chabazite, and ferrierite. ¹¹

Azo dyes are the most important synthetic dyes with -N=N- bonds in their molecular structure. They can be classified according to number of azo groups, such as monoazo, diazo, triazo, polyazo, and azoic.¹²

Direct black 22 (DB-22) is one of the tetra azo dyes used in textile industry for dyeing cellulosic fibers such as cotton, wool, viscose, rayon, and paper. The high concentration of DB-22 in wastewater harms the environment with its carcinogenic properties, toxicity, organic matter content, and strong

color.¹³ For this reason, wastewater containing DB-22 should be released to the environment after being treated. There are few studies in the literature on DB-22 removal. In their study, Hien et al. 13 investigated the catalytic ozonation of DB-22 using different metal slags. Carvalho et al. 14 examined the removal of DB-22 using microaerated upflow anaerobic sludge blanket (UASB) reactors. Gomes et al. 15 investigated the degradation of DB-22 using homogeneous and heterogeneous photo-Fenton advanced oxidation process. They used LED light as a source of radiation, and ferrous sulfate and iron residue as catalysts. In another study, Menezes et al. 16 investigated the effect of the combination of anaerobic process and micro-aeration (continuous and intermittent) on DB-22 removal. Shu et al.¹⁷ examined the decolorization of DB-22 using the UV/H₂O₂ process, ozonation, and pre-ozonation coupled with UV/H₂O₂. Moreover, some other studies focused on the photoelectrochemical oxidation of DB-22 under elevated oxygen pressure and the adsorption of DB-22 using polymeric adsorbent. 18,19 The aim of this study is to investigate photo-Fenton like oxidation of DB-22 using zeolite modified zinc ferrite. Kinetic and thermodynamic properties of the DB-22 decolorization and the effects of the reaction parameters such as catalyst modification with HCl, catalyst amount, H₂O₂ amount, salt addition, pH, initial dye concentration, temperature were also investigated. The zeolite and synthesized catalysts were characterized using FTIR, SEM, EDS and XRD.

82 83

84

85

86

87

88

89

90

96

97

98

99

67

68

69

70

71

72

73

74

75

76

77

78

79

80

81

2. Materials and Methods

2.1. Materials and Equipments

The zeolite with a particle size of 23 μ was procured from a company in Balıkesir, Turkey. It was a commercial product and used without purification. HCl and NaOH were procured from Tekkim, DB-22 (commercial name Direct Black 22 VSF 1600) from a company named "HNY" in Turkey, H₂O₂ (34.5-36.5 w/w %, Cas no: 7722-84-1) from Sigma, CaCl₂ from Emir Kimya, FeSO₄7H₂O (Cas no: 7782-63-0) from Merck and ZnSO₄7H₂O (Art no: 8881) from Merck.

A magnetic stirrer (HSD-180), pH meter (C561, Consort), digital scale (Ohaus), centrifuge (Nuve, NF 200), and incubator (Ecocell) were used in the study. UV- spectrophotometer (Hach, DR-2400) was used to measure the absorbance of the sample. A COD reactor (Hach DRB 200) was used to heat the samples before measuring the COD value. A UV lamp (Light Tech GPH212T5L/4, 10 W) with a wavelength of 254 nm was used in the photocatalytic decolorization of DB-22.

2.2. Preparation of the Catalyst

The catalyst, zeolite/Zn/Fe was prepared by chemical coprecipitation method. First, iron II sulphate heptahydrate (FeSO₄.7H₂O) and zinc sulphate heptahydrate (ZnSO₄.7H₂O) with a molar ratio of 2:1 were dissolved in 200 ml distilled water. Then, zeolite was added to the solution and heated to 65-70

°C while stirring with a magnetic stirrer. The mixture was stirred for 30 min using a magnetic stirrer. 3 M NaOH solution was added dropwise to the solution, and pH of the solution was adjusted to 12. After addition of NaOH solution, stirring was continued for one hour at 100 °C. The prepared catalyst was left for one day at room conditions, and then placed in water bath for 4 h at 95 °C. After that, it was dried at 95 °C for 90 h. The dried composite was soaked in 0.1 N HCl solution at room temperature for 24 hour, and then filtered and washed using distilled water. Finally, it was dried at 95 °C for 60 hours. The catalysts treated with and without HCl were coded as m-ZZF and ZZF, respectively.

2.3. Characterization

The catalyts used in the study were characterized by XRD, FTIR, SEM and EDS. The crystalline structure of the samples was determined by XRD analysis using Rigaku Smart Lab with Cu-Kα radiation at 40kV and 30mA. The samples were scanned from 5°- 90° at a rate of 2°/min, and with a step size of 0.01. FTIR (PerkinElmer, Spectrum Two) was used to identify the functional groups of the adsorbents before and after adsorption in the range of 400-4000 cm⁻¹. SEM and EDS analysis were performed using Tescan, MAIA3 XMU.

2.4. Experimental

In the study, a cylindrical glass reactor with a volume of 250 ml, a height of 20 cm, and a diameter of 5 cm was used. The reactor was filled with 200 ml of DB-22 solution with a known concentration, and the catalyst was added, then magnetically stirred for 30 min in the dark to ensure a complete equilibration of adsorption/desorption of DB-22 on the catalyst surface. In order to find the amount of dye adsorbed on the catalyst surface in the dark, a sample was taken from the dye solution and its absorbance was measured. Then, a UV lamp with a quartz tube was placed in the center of the reactor at a distance of 2 cm from the bottom. The surface of the reactor was covered with aluminum foil to prevent light penetration. While the DB 22 solution was stirred continuously, the UV lamp was switched on and the reaction time was started immediately. Stirring rate was kept constant at 800 rpm in all experiments. The experiments were carried out at the original pH of the dye solution, except for the experiments in which the pH effect was examined. The samples taken from the reactor at regular intervals were centrifuged at 5000 rpm for 10 minutes. Then, the absorbance of the dye solution was recorded at 481 nm using UV-spectrophotometer to calculate decolorization. Decolorization of DB-22 dye was calculated using the Eq. 1

130 Decolorization,
$$\% = \frac{(C_0 - C)}{C_0} * 100$$
 (1)

where, C_o and C represent the concentration of the DB-22 at the beginning of the reaction and at corresponding time, respectively.

COD was measured using Hach DR 2400 spectrophotometer, Hach COD reactor and test kits in the range 0-1500 ppm. Instructions for the Hach higher range test followed.

The DB-22 solution temperature was not controlled in the experiments. The reaction was started at a room temperature of 25 °C, except for the experiments in which the effect of temperature was examined, and a temperature increase of 15 °C was observed at the end of 60 minutes. No temperature control was done to constitute a natural environment and to save on cooling water cost.

3. Results and Discussion

3.1. Catalyst Characterization

The XRD pattern of the zeolite (Z) and m-ZZF are shown in Fig.1. As can be seen in the Fig.1, all diffraction peaks were apparent and strong. This indicates that the Z and m-ZZF samples were in crystalline form.

According to XRD data, zeolite (Z) was identified by its characteristic X-ray diffraction peaks at 20: 11.15°, 16.87°, 20.84°, 22.34°, 22.73°, 26.02°, 26.6°, 29.85°. These XRD peaks of the Z coded sample are compatible with the clinoptilolite with PDF card no 00-013-0304. This result shows that the zeolite was composed of clinoptilolite. As shown in Fig.1-b, all peaks of natural zeolite accept 26.74° disappeared after the preparation of m-ZZF. According to the PDF card, peaks appear at 34.96°, 52.74° and 61.97° matchwell with PDF card 00-010-0467 (Franklinite, ZnFe₂O₄). Spinel ferrite ZnFe₂O₄ coats the surface of zeolite. This improves the photocatalytic activity of m-ZZF.

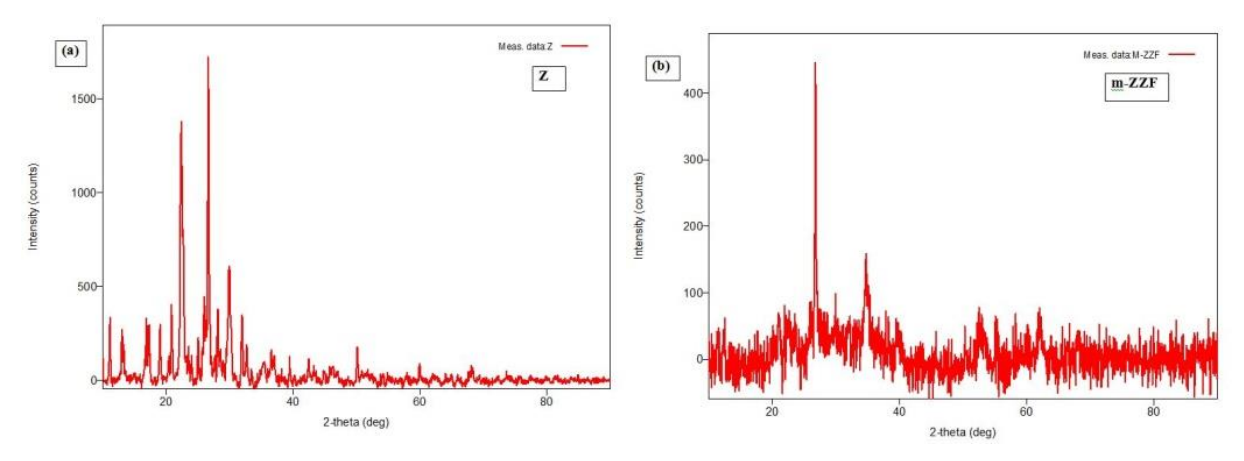


Fig. 1. XRD analysis of (a) Z and (b) m-ZZF

Figure 2 shows the SEM images and EDS results of zeolite (Z) and m-ZZF. As can be seen in SEM image of Z, particles had an irregular shape and porous surface. In m-ZZF image, zinc ferrite

agglomerated on the surface of the zeolite. According to EDS results, zeolite was mainly composed of O, Si, and Al, in addition to small amounts of K, Mg, Ca and Fe. The percentage of iron and zinc considerably increased in m-ZZF.

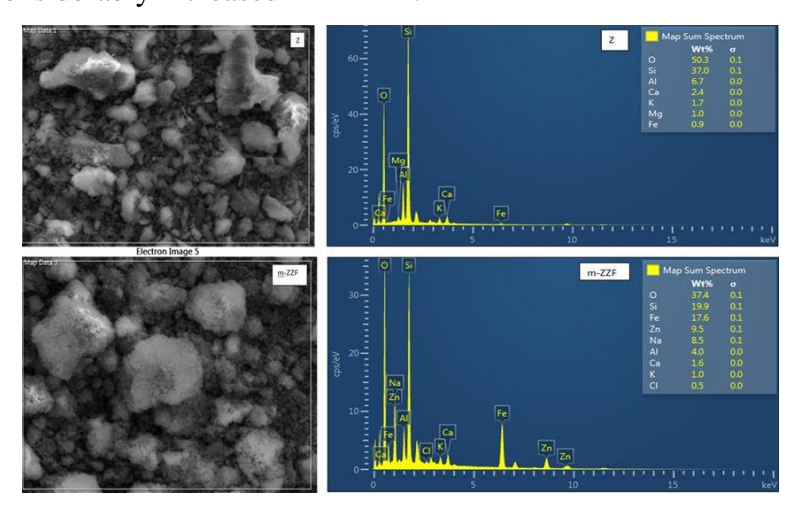


Fig. 2. SEM image and EDS results of zeolit and m-ZZF

Figure 3 shows the FTIR spectra of zeolite, ZZF, m-ZZF, and m-ZZF after being used in DB-22 decolorization. As can be seen in Fig. 3, the zeolite had bands around 800, 1030, and 1630 cm⁻¹. The band between 450 and 1100 cm⁻¹ was related to the active zeolite lattice bands.²⁰ The band at 800 cm⁻¹ corresponds to the stretching vibration of Si-O-Si. The absorption bands around 1030 cm⁻¹ were due to asymmetric stretching vibrations of Al and/or Si bonding with oxygen. The peak at 1030 cm⁻¹ is the proof that the zeolite was composed of alumina silicate. The peak at 1030 cm⁻¹ is sensitive to the change in Si and Al content. The band at 1630 cm⁻¹ is related to the O-H stretching vibrations and the adsorbed H₂O molecules.²⁰⁻²³ As seen in Fig. 3, there were a few differences between Z, ZZF, and m-ZZF spectrum. In ZZF and m-ZZF, the peaks at 800 cm⁻¹ and 1630 cm⁻¹ disappeared. The peak at 1000 cm⁻¹ in m-ZZF was the result of the shift of the peak at 1030 cm⁻¹ in Z, and the transmittance at 1000 cm⁻¹ increased. With the addition of zinc ferrite to the structure of the zeolite, the ratio of Al and Si changed. Maybe that is why, the transmittance increased. The FTIR spectrum of m-ZZF after it was used in DB-22 decolorization was similar to that before it was used and only the transmittance at 1000 cm⁻¹ decreased.

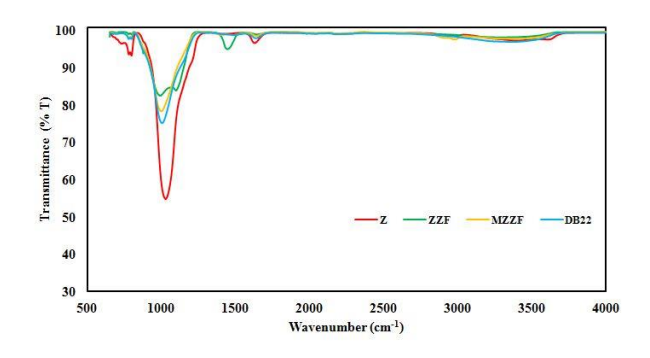
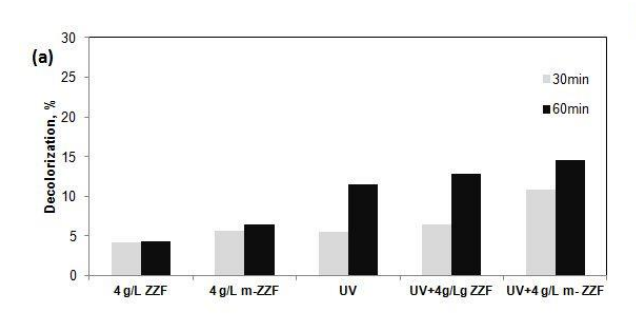


Fig. 3. FTIR analysis of the Z, ZZF, m-ZZF and m-ZZF after being used in DB-22 decolorization

3.2. The effect of HCl Modification of Catalyst on Photocatalytic Decolorization of DB-22

In order to determine the effective catalyst in the photocatalytic degradation of DB-22, the experiments were performed under the following reaction conditions: initial dye concentration: 0.04 g/L, catalyst loading: 4 g/L, original pH, and UV lamp. As seen in Fig. 4-a, in the presence of ZZF and m-ZZF, the decolorization rate was higher with using UV lamp than without UV lamp. The catalyst modified with HCl (m-ZZF) gave better results than ZZF. Mesopores formed as a result of acid treatment of zeolite are active surfaces for the adsorption and catalysis of relatively large molecules. The decolorization of DB-22 using UV light and 4 g/L m-ZZF was 10.9% and 14.6% at the end of 30 min and 60 min, respectively. On the other hand, a decolorization of 6.4% and 12.8% was observed in the experimental set up with UV light and 4 g/L ZZF at the reaction times of 30 min and 60 min respectively. So, the decolorization rate increased in the system using UV light and m-ZZF. Considering the individual m-ZZF and UV processes, it is seen that the photocatalytic activity of m-ZZF is very poor.



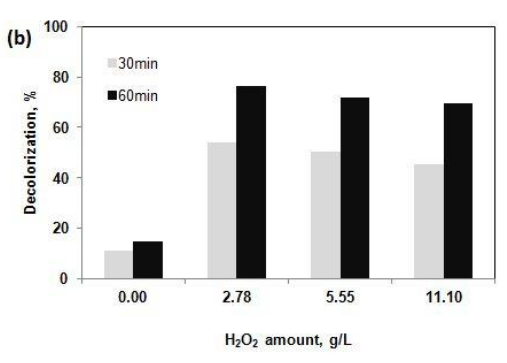


Fig. 4. Effect of (a) HCl modification of catalyst (initial dye concentration: 0.04 g/L, initial temperature: 25 °C, catalyst amount: 4 g/L, original pH) and (b) H_2O_2 concentration (initial dye concentration: 0.04 g/L, initial temperature: 25 °C, m-ZZF amount: 4 g/L, original pH, UV light) on the decolorization of DB-22

3.3. Effect of Hydrogen Peroxide Amount

The effect of hydrogen peroxide amount on the decolorization of DB-22 was studied with the H_2O_2 amounts of 2.78 g/L, 5.55 g/L, and 11.1 g/L while keeping all other parameters constant (initial DB-22 concentration: 0.04 g/L, m-ZZF amount: 4 g/L, UV light, and original pH). The results are presented in Fig. 4-b. As seen in Fig. 4-b, the decolorization of DB-22 without the addition of H_2O_2 was less than that with the addition of H_2O_2 . The photocatalytic decolorization of the DB-22 enhanced when the H_2O_2 amount was introduced to the Fenton system due to the accelerated generation of hydroxyl radicals (OH•). According to our results, the decolorization rate decreased with increasing H_2O_2 concentration. In 60 min, the decolorization rate increased from 69.5% to 76.4% when the H_2O_2 concentration decreased from 5.55 g/L to 2.78g/L.

At high H₂O₂ concentrations, excess hydrogen peroxide reacts with the produced OH• radicals and causes the formation of less reactive radicals like hydrogen dioxide.^{21,25} The reactions between OH• radicals and excess hydrogen peroxide are given by the equations below²⁶:

$$OH^{\bullet} + H_2O_2 \rightarrow HO_2^{\bullet} + H_2O$$
 (2)

213
$$HO_2 \cdot + OH \cdot \rightarrow O_2 + H_2O$$
 (3)

$$OH + OH \bullet \rightarrow H_2O_2 \tag{4}$$

A similar result was reported by Abharya et al.²⁴ They reported that photocatalytic degradation decreased after the H₂O₂ concentration of 0.0389 M and when the amount of H₂O₂ was above the critical value, the reaction between excess H₂O₂ and the generated OH• radicals caused a decrease in photocatalytic activity over time. In another study, Badvi and Javanbakht²¹ reported similar results for the photocatalytic degradation of methylene blue. They found that the dye degradation decreased when the H₂O₂ concentration was increased from 250 to 750 mg/L. Moreover, they asserted that when H₂O₂ concentration exceeded a certain level, hydrogen peroxide acted as a scavenger of the photo produced holes and caused a decrease in the efficiency of dye degradation.

3.4. Effect of Catalyst Amount

In order to examine the effect of the amount of catalyst and to find the optimum amount of catalyst, experiments were carried out by changing the amount of catalyst between 1 g/L and 6 g/L while keeping the other parameters constant (H₂O₂ amount: 2.78g/L, initial DB-22 concentration: 0.04 g/L, UV light, original pH and initial temperature: 25 °C). The results are presented in Fig. 5-a.

As can be seen in Fig. 5-a, as the catalyst amount was increased from 1g/L to 3 g/L, the decolorization rate of DB-22 increased from 78.0% to 80.8%. After the catalyst loading of 3 g/L, the decolorization rate decreased. Under the studied conditions, the optimum catalyst amount was found to be 3 g/L. This means that, the catalyst amounts higher than the optimum value may decrease the

light transmittance. Abharya et al.²⁴ investigated the photocatalytic treatment of methylene blue and obtained similar results. They reported that the number of reactive sites increased with increasing catalyst loading and after the optimum catalyst amount, the catalyst particles tended to agglomerate, causing a decrease in the number of reactive sites and an increase in light scattering. In another study, Gan and Li²⁷ investigated the decolorization of Rhodamine B using catalyst by Fenton like process. They reported that the decolorization of Rhodamine B increased with increasing the catalyst amount from 0.5g/dm³ to 1g/dm³, but after 1g/dm³, it started to decrease. They also reported that, after the optimum catalyst amount (1 g/dm³), the catalyst surface area decreased due to the aggregation between particles, and as a result, color removal decreased. Ejhieh and Khorsandi¹ investigated the photocatalytic decolorization of Eriochrome Black T using NiS-P zeolite. They reported that the decolorization of Erichrome Black T increased with increasing the catalyst amount from 0.1 g/L to 0.8 g/L, but after 0.8 g/L, it started to decrease. They asserted that as the amount of catalyst increased, the solid particles blocked the photon penetration. In another study, Ji et al.28 investigated the decolorization of methylene blue using catalyst and heterogeneous photo Fenton system and reported that the decolorization of methylene blue increased with increasing the catalyst from 0.25 to 1.5 g/L. As the amount of catalyst increases, the number of active sites increases. In the catalyst amounts higher than 1.5 g/L, the catalyst particles prevented the transmission of UV light into the solution. Therefore, with the increase of the amount of catalyst from 1.5 to 2 g/L, the rate of decolorization decreased.

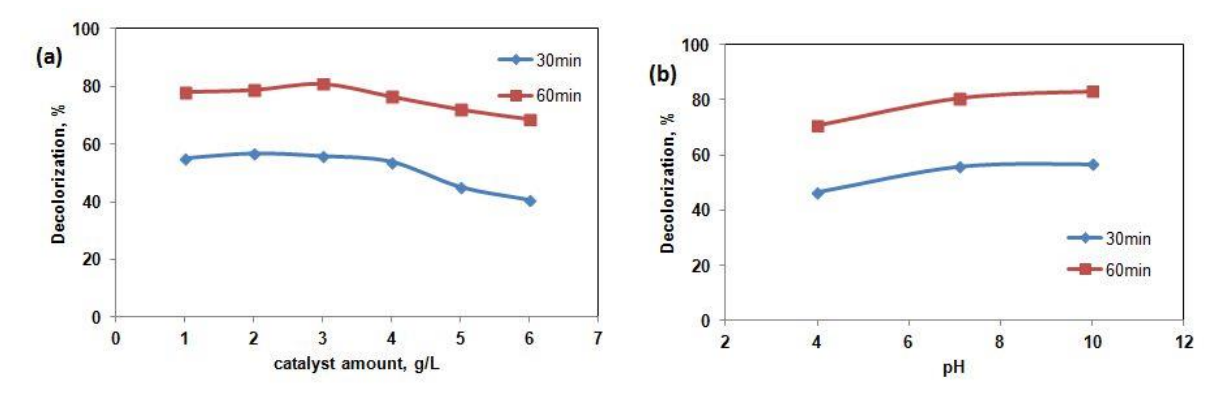


Fig. 5. Effect of (a) m-ZZF amount (initial dye concentration: 0.04 g/L, initial temperature: 25 °C, original pH, H_2O_2 amount 2.78 g/L, original pH, UV light) (b) pH (initial dye concentration: 0.04 g/L, initial temperature: 25 °C, H_2O_2 amount 2.78 g/L, m-ZZF amount: 3 g/L, UV light) on the decolorization of DB-22

3.5. Effect of Initial pH

232

233

234

235

236

237

238

239

240

241

242

243

244

245

246

247

248

249

250

251

252

253

254

255

256

257

The effect of pH on the decolorization of DB-22 was studied at the initial pHs of 4, \approx 7.1, and 10. \approx 7.1 is the original pH of the dye solution. The pH of the DB-22 solution was adjusted at the beginning of the experiment. pH control was not done during the reaction. Fig. 5-b shows the results.

The decolorization of DB-22 increased when the pH was increased from 4 to 10. The decolorization of DB-22 was found to be 70.8%, 80.2%, and 83.3% at the pH values of 4, 7.1, and 10 respectively. Karimi-Shamsabadi et al.²⁹ obtained similar results for the photocatalytic degradation of Erichrome black T using NiO-ZnO doped nanozeolite X. They reported that at the basic pH, due to higher concentration of hydroxyl ions, the concentration of hydroxyl radicals increased, which enhanced the photocatalytic degradation rate. In another study by Ejhieh and Khorsandi¹, it was asserted that the degradation of Erichrome Black T increased with increasing the initial pH. Under the acidic conditions, Cl⁻ ions and hydroxyl radicals combine to form inorganic radical ions (ClO⁻•). They reported that the reactivity of ClO⁻• anions was less than that of hydroxyl radicals, therefore, these radicals did not involve in the decolorization reactions. Under basic conditions, due to the increase in the number hydroxyl radicals, the decolorization rate increased.

3.6. Effect of Salt Addition

The effect of salt on the decolorization of DB-22 was investigated using CaCl₂. The results obtained for different CaCl₂ amounts are given in Fig. 6. As can be seen in Fig. 6, the decolorization rate of DB-22 increased with the addition of CaCl₂. When the CaCl₂ amount was increased from 2.5 to 5 g/L, no significant change was observed in the decolorization rate at the reaction time of 60 min. In the reaction time of 30 min, while the decolorization of DB-22 was found to be 83.2% in the case of the addition of 2.5 g/L CaCl₂, it was 90.1% in the case of the addition of 3.75 g/L CaCl₂. 3.75 g/L CaCl₂ was chosen due to the higher decolorization rate at 30 min. The results show that m-ZZF is effective in the presence of CaCl₂.

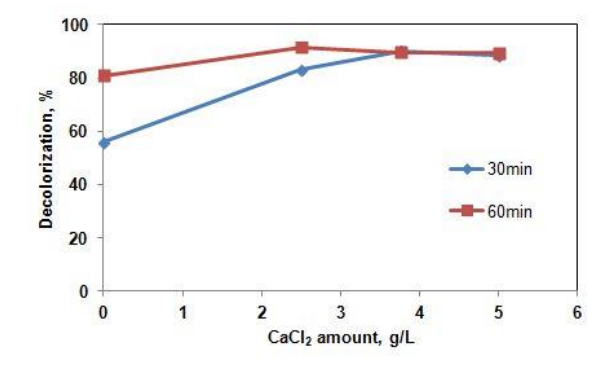


Fig. 6. Effect of CaCl₂ amount on the decolorization of DB-22 (initial dye concentration: 0.040 g/L, initial temperature: 25 °C, original pH, H₂O₂ amount: 2.78 g/L, m-ZZF amount: 3 g/L, UV light)

Gan et al.²⁷ reported similar results in their study investigating the effect of ionic strength using different concentrations of NaCl. According to their results, increasing NaCl from 0.05 M to 0.1M did not change the degradation rate. The ionic strength for the adsorption of dye on oxide surface can influence the electrostatic interactions between the oxide surface and the dye species. In heterogeneous catalytic systems, the presence of excess anions may affect the equilibria between the dye molecules and the catalyst surface.²⁷

When low concentrations of salt are used, Cl• radicals with high oxidizing potential are formed and they oxidize organic materials. Cl• radicals have a high affinity for a hole and they can also prevent electron-hole recombination, thus enhancing the efficiency of reactive species formation. If the salt amount is more than the optimum value, the dye removal efficiency decreases. This is because the Cl⁻ competes with the dye molecules for the limited catalyst surface and the surface is deactivated.³⁰

3.7. Effect of Initial Dye Concentration and Reaction Time

In the study, the effects of initial dye concentration and reaction time on DB-22 decolorization were also investigated. The experiments were done within the initial concentration range of 0.025-0.070 g/L with a m-ZZF amount of 3 g/L, H_2O_2 amount of 2.78 g/L, and $CaCl_2$ amount of 3.75 g/L, at original pH, at an initial temperature of 25 °C and under UV light. Fig. 7 shows the effect of initial dye concentration and reaction time on the decolorization of DB-22.

The experimental results showed that the decolorization rate of DB-22 was faster in the first 10 min. After 10min, decolorization rate slowed down and remained almost constant after the reaction time of 30 min. As seen in Fig. 7, the decolorization of DB-22 increased with the increasing initial concentrations. The decolorization of DB-22 for the reaction time of 60 min was found to be 81.3%, 90.2%, 90.5%, 91%, and 93.3% at the initial dye concentrations of 0.025, 0.040, 0.050, 0.060, and 0.070 g/L, respectively. In the literature, Ejhieh and Khorsandi¹ reported similar results for the photocatalytic decolorization of Eriochrome Black T using NiS-P zeolite. They found that the decolorization of Erichrome Black T increased with increasing the initial concentration from 10 mg/L to 40 mg/L. Having a lifetime as short as a few nanoseconds, hydroxyl radicals react immediately after formation. As the number of dye molecules per unit volume increases, so does the probability of collisions between organic matter and oxidizing species. As a result, decolorization rate increases. In their study, Gan and Li²⁷ found that the decolorization of Rhodamine B increased with increasing the initial concentration from 2.5 to 50 mg/L using ricehull based silica supported catalyst by Fenton like process. The probability of collision between dye molecules and near-surface activating species increases with the increase of dye concentration per volume.

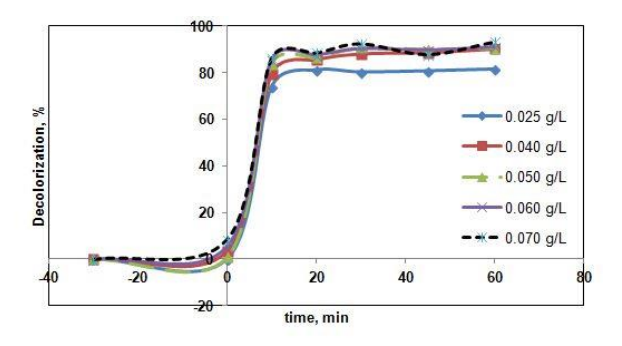


Fig. 7. Effect of initial dye concentration on the decolorization of DB-22 (pH: original, initial temperature: 25 °C, H₂O₂ amount: 2.78 g/L, m-ZZF amount: 3 g/L, CaCl₂ amount: 3.75 g/L, UV light)

3.8. Effect of Temperature

The effect of temperature on the decolorization of DB-22 was investigated at 25 °C, 35 °C, and 45 °C while keeping other parameters constant (initial concentration of dye: 0.040 g/L, initial pH: original, H₂O₂ amount: 2.78 g/L, m-ZZF amount: 3 g/L, CaCl₂ amount: 3.75 g/L, UV light). As mentioned in the experimental section, the experiments were performed without cooling, and a temperature increase was observed. Initial decolorization rate was calculated for the reaction time of 10 min. An increase of 2°C from the initial temperature was observed in 10 min.

Figure 8 shows the effect of temperature on the initial decolorization rate. As can be seen in Fig. 8, the initial decolorization of DB-22 in 10 min decreased with increasing temperatures. The decrease in the decolorization rate with the increasing temperatures shows that the reaction occurred under exothermic conditions. An increase in the reaction temperature causes a decrease in the oxygen solubility in the solution. The rate of electron withdrawal from the surface of the photocatalyst decreases due to the decrease in dissolved oxygen concentration. Andreozzi et al. investigated the effect of temperature on the photocatalytic degradation of 4-nitrophenol and reported that temperature had a negative effect on the degradation at pH 3. The presence of oxygen is important to keep high the concentration of photogenerated OH• radicals on the surface of the catalyst. The concentration of the photogenerated holes decreases due to the decrease in oxygen solubility at high reaction temperatures.

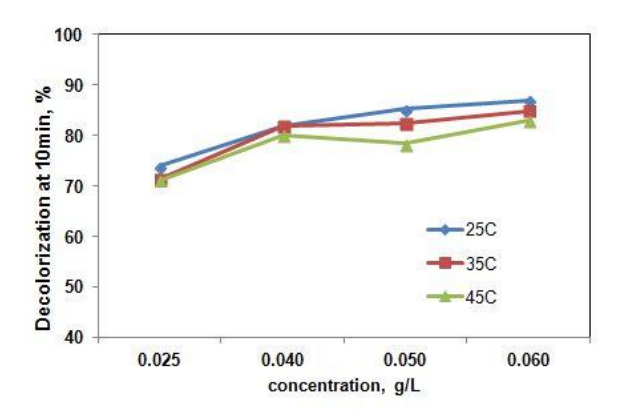


Fig. 8. Effect of temperature on the initial decolorization rate of DB-22 (initial pH: original, H₂O₂ amount: 2.78 g/L, m-ZZF amount: 3 g/L, CaCl₂ amount: 3.75 g/L, UV light)

3.9. Decolorization of DB-22 using Different Processes

Decolorization of DB-22 was investigated at 0.040g/L initial dye concentration and $25^{\circ}C$ initial temperature using different processes. The results are given in Fig. 9. Decolorization rate using 3 g/L m-ZZF and (3 g/L m-ZZF + 2.78 g/L $_{202}$) processes were 2.4% and 5.7% respectively. The effect of UV light was studied using processes such as, $_{32}$ L m-ZZF, $_{202}$ L $_{202}$ CaCl₂ and (3 g/L m-ZZF + 2.5 g/L $_{202}$ CaCl₂). Decolorization of (UV + 3 g/L m-ZZF + 2.5 g/L $_{202}$ CaCl₂) process was greater than that of the individual processes such as UV, (UV + $_{202}$ C m-ZZF) and (UV + $_{202}$ CaCl₂). Decolorization rate was 76.1% at 30 min and 82.3% at 60 min using (UV + 3 g/L m-ZZF + 2.5 g/L $_{202}$ CaCl₂) process. To identify the effect of the $_{202}$ CaCl₂, experiments were also done using (UV + 2.78 g/L $_{202}$ CaCl₂), (UV + 2.78 g/L $_{202}$ CaCl₂) and (UV + 2.78 g/L $_{202}$ CaCl₂). (UV + 2.78 g/L $_{202}$ CaCl₂) and (UV + 2.78 g/L $_{202}$ CaCl₂) processes provided nearly the same decololorization rate as 82% at 60 min. Decolorization rate at 60 min using (UV + 2.78 g/L $_{202}$ CaCl₂) process was found to be 91.5%.

The decolorization of DB-22 for the reaction time of 30 min was found to be 76.1% at (UV+ 3 g/L m-ZZF + 2.5 g/L CaCl₂) process. Addition of H₂O₂ increased the color removal and decolorization of DB-22 at 30 min was found to be 83.2% at (UV + 2.78 g/L H₂O₂ + 3 g/L m-ZZF + 2.5 g/L CaCl₂) process. With increasing CaCl₂ amount from 2.5 to 3.75 g/L, decolorization rate increased from 83.2% to 90.1% in 30 min reaction time. With the synergetic effect of UV, m-ZZF, H₂O₂ and CaCl₂, the highest color removal was achieved in 30 minutes. Ionic strength effects the electrostatic interaction between the catalyst surface and dye molecules. Addition of anions might allow the neutralization of the positive sites on catalyst surface. Nonelectrostatic interaction between dye molecules and neutral sites could occur due to van del Walls forces or low energetic H-bonds.²⁷ According to Sudrajat and

Babel³⁰, the Cl• radicals formed as a result of the surface chain transfer reaction of the chlorine ion oxidizes the organic compounds.

Considering these results, the possible decolorization mechanism of DB-22 over m-ZZF may consist of the following steps: Due to the non-electrostatic interaction between the dye molecules and the neutral sites, dye molecules may be adsorbed on the catalyst surface in the presence of Cl⁻ ions.²⁷ Electron/hole pairs are generated on the m-ZZF surface under UV light. Electrons on m-ZZF react with H₂O₂ to produce both OH⁻ ions and OH• radicals. Photogenerated holes could react with OH⁻ ions or adsorbed water to generate OH• radicals.^{33,34} In the presence of salt, the Cl• radicals could oxidize dye molecules.³⁰ The generated radicals react with DB-22 and degradation products are formed.

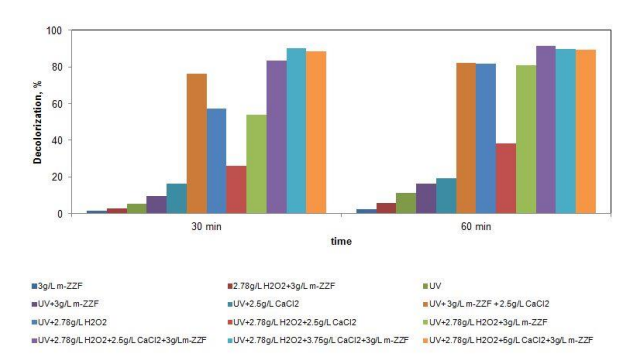


Fig. 9. Comparison of different processes

3.10. COD Removal

The COD value represents the amount of oxygen required for oxidation of organics into CO₂ and water. It is related with total organic compounds in the wastewater. In the study, the variation of COD with time was investigated under the following reaction conditions: initial dye concentration: 0.04 g/L, m-ZZF amount: 3 g/L, H₂O₂ amount: 2.78 g/L, CaCl₂ amount 3.75 g/L, original pH, and UV lamp. As seen from Fig. 10, COD removal increases with increasing time. 26.9% COD removal was obtained at the end of 60 min reaction time. While the decolorization of DB-22 was found to be 79.5% and 90.1% at the 10 min and 30 min reaction time respectively, low COD removal was achieved under the studied conditions. COD removal showed the partial oxidation of the organic pollutants to CO₂ and H₂O. The colorless intermediates were formed as a result of DB-22 oxidation. These intermediates cause low COD removal.³⁴ According to results, photo-Fenton like process is more useful for decolorization of DB-22 than COD removal.

The operating cost of the photo-Fenton process includes cost of chemicals and energy. Electricity is used in the UV lamb and mixing the process. According to Çalık³⁵, operating cost of the photo-Fenton

process changed between 13.46-20.13 €/m³ for the used chemicals and electrical energy for treatment of textile wastewater.

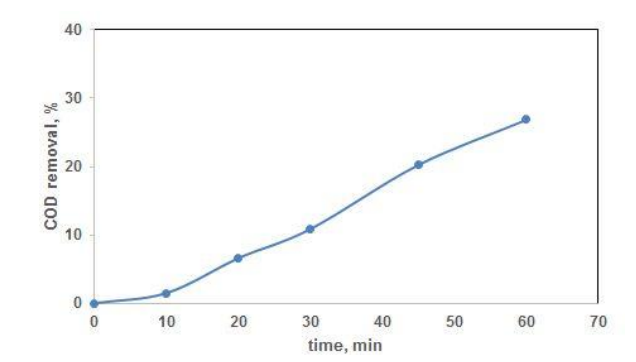


Fig. 10. Variation of COD with time (initial dye concentration: 0.04g/L, pH: original, initial temperature: 25 °C, H₂O₂ amount: 2.78 g/L, m-ZZF amount: 3 g/L, CaCl₂ amount: 3.75 g/L, UV light)

3.11. Kinetic and Thermodynamic Studies

The initial rate equation for decolorization of dye is as follows:

$$r_o = \left(-\frac{dc}{dt}\right)_o = k_{app} C_o^{\ n} \tag{5}$$

where k_{app} is the overall observed rate constant for the reaction, n is the order of the reaction with respect to concentration. Eq. 5 is linearized by taking the natural logarithm and Eq. 6 is obtained.

$$\ln(r_0) = \ln k_{app} + n \ln C_0 \tag{6}$$

If $ln(r_0)$ is plotted against lnC_0 , the slope of the straight line gives the degree of reaction (n) and intercept gives the lnk_{app} value. Fig. 11 shows the plot of $ln(r_0)$ against lnC_0 for 25 °C, 35 °C, and 45 °C. The initial decolorization rate of DB-22 was calculated for the initial 10 min. The calculated n and k_{app} values were listed in Table 1. A high regression coefficient indicates a good compatibility. The values of n were 1.08, 1.12, and 1.16 at 25 °C, 35 °C and 45 °C respectively. It can be said that, the reaction order of the photocatalytic decolorization of DB-22 was 1.1 under the studied conditions.

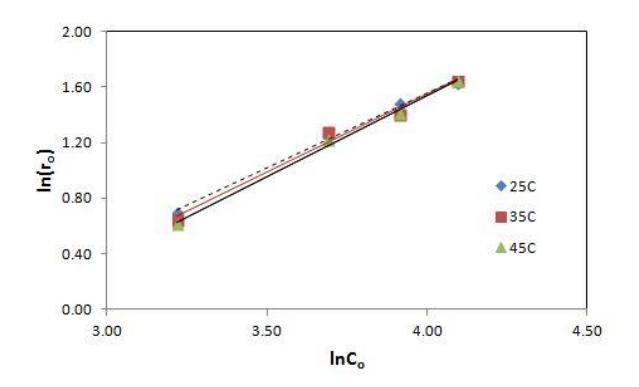


Fig. 11. ln(r_o) versus lnC_o (initial pH: original, H₂O₂ amount: 2.78 g/L, m-ZZF amount: 3 g/L, CaCl₂ amount: 3.75 g/L, UV light)

Table 1. The reaction orders and rate constants

T(K)	n	$\mathbf{k_{app}} (\text{mg/L})^{-0.1}/\text{min}$	\mathbb{R}^2
298	1.08	0.064	0.9946
308	1.12	0.053	0.9847
318	1.16	0.044	0.9949

The activation energy of the reaction was calculated using Arrhenius equation³⁶.

$$k_{app} = A e^{-Ea/RT}$$
 (7)

where k_{app} is the apparent reaction rate constant, A is the Arrhenius factor, E_a is the activation energy (J/mol), R is the ideal gas constant (8.314 J/molK), and T is the temperature (K). The logarithmic form of Eq. 7 can be written as:

$$\ln k_{app} = \ln A - E_a / RT \tag{8}$$

When $\ln k_{app}$ is plotted against 1/T, the slope gives $-E_a/R$. The Arrhenius plot is presented in Fig. 12-a. Activation energy, E_a was calculated to be -14.76 kJ/mol under the studied conditions. This result showed that the decolorization rate decreased with increasing temperature, as mentioned in the section 3.4. The activation energy is the minimum energy required to break the bonds of the species participating in the reaction and to form new bonds. A low activation energy indicates that less energy is required to break bonds.³⁷

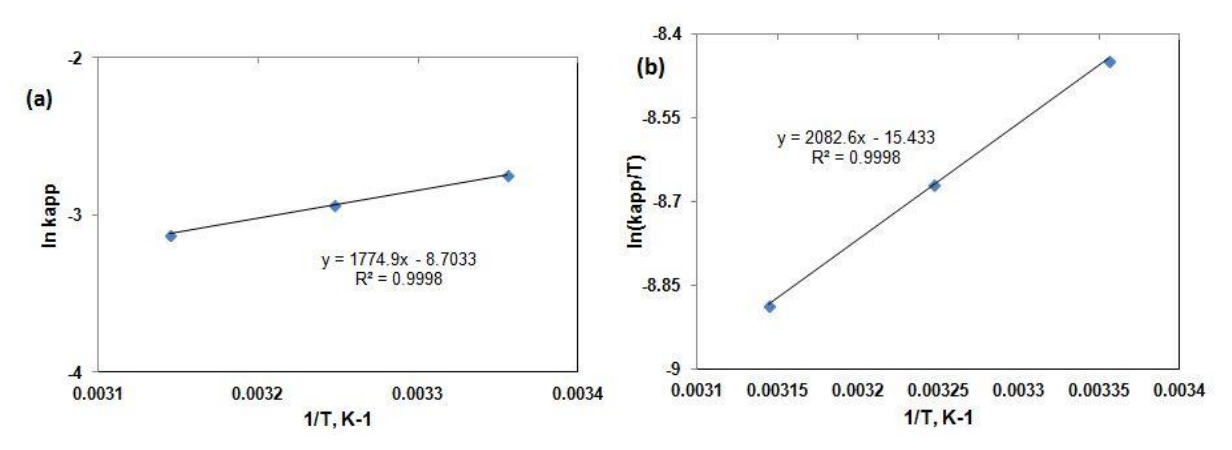


Fig. 12. (a) Arrhenius plot of lnk_{app} against 1/T (b) $ln\frac{k_{app}}{T}$ versus 1/T

The activation enthalpy (ΔH^0) and the activation entropy (ΔS^0) were calculated by plotting $ln(k_{app}/T)$ against 1/T according to the equation below²⁷:

$$ln\frac{k_{app}}{T} = ln\frac{R}{N_A h} + \frac{\Delta S^0}{R} - \frac{\Delta H^0}{RT}$$
(9)

where N_A is Avogadro constant (6.022*10²³ mol⁻¹) and h is Planck constant (6.626*10⁻³⁴ Js).

The slopes of this line gives $-\Delta H^0/R$ and the intercept gives $ln\frac{R}{N_Ah} + \frac{\Delta S^0}{R}$. Fig. 12-b shows the plot of $ln\frac{k_{app}}{T}$ vs 1/T. The reaction enthalpy was calculated to be -17.31 kJ/mol. The sign of the enthalpy indicates an exothermic reaction. The value of activation entropy was calculated as -0.326 kJ/molK. The negative value of ΔS^0 indicated that the photocatalytic decolorization of DB-22 was less random and the transition state formed in the degradation process had a lower structural freedom compared to the reactants, and this also confirms that the process was irreversible. 37,38

The lowest absolute values of E_a , ΔH^0 , and ΔS^0 found for the catalyst used in the study are indicative of its highest catalytic activity. According to the literature, the value of the activation energy determines whether the reaction is diffusion or reaction rate controlled. If the activation energy is lower than 29 kJ/mol, this indicates that the reaction is controlled by diffusion process. ^{39,40} In this study, a low activation energy was obtained; so it can be said that the photocatalytic decolorization of DB-22 using m-ZZF was a diffusion controlled process.

The standard Gibbs free energy was calculated using Eq. $10^{36,38}$

$$\Delta G^0 = \Delta H^0 - T \Delta S^0 \tag{10}$$

Table 2 gives the thermodynamic parameters. As can be seen in Table 2, standard Gibbs free energy change (ΔG^0) had a positive value and it increased with increasing temperatures. This result indicated no spontaneous processes and weak adsorption of dye molecules on m-ZZF.³⁶

Table 2. Kinetic and thermodynamic parameters of the photocatalytic degradation of DB-22

T	$\mathbf{k}_{\mathrm{app}}$	Ea	ΔH^0	ΔS^0	ΔG^0
(K)	$(mg/L)^{-0.1}/min$	(kJ/mol)	(kJ/mol)	(kJ/molK)	(kJ/mol)
298	0.064	-14.76	-17.31	-0.326	84.02
308	0.053				87.28
318	0.044				90.36

467 4. Conclusions

In this study, decolorization of Direct Black 22 was investigated using photo Fenton-like method. UV lamp was used as a source of light. Zeolite modified with zinc ferrite (m-ZZF) was used as a heterogeneous catalyst. m-ZZF was prepared by coprecipitation method. The zeolite and m-ZZF were characterized using XRD, SEM, EDS, and FTIR analysis. Zeolite surface was successfully coated with zinc ferrite.

The results showed that under UV light, the decolorization of DB-22 was higher with m-ZZF than with ZZF. The effect of various parameters (initial pH, initial dye concentration, catalyst amount, hydrogen peroxide concentration, CaCl₂ amount, temperature) on the DB-22 decolorization was analysed, kinetic and thermodynamic investigations were performed as well. The decolorization of DB-22 was found to be 93.3% under the following reaction conditions: initial concentration: 0.070 g/L, initial temperature: 25 °C, original pH, H₂O₂ amount: 2.78g/L, m-ZZF amount: 3 g/L, CaCl₂ amount 3.75 g/L, reaction time: 60 min, and under UV light. The activation energy was found to be -14.76 kJ/mol. The decolorization reaction was exothermic and the calculated reaction enthalpy was -17.31 kJ/mol. The value of activation entropy was calculated to be -0.326 kJ/mol. The standard Gibbs free energy change of activation had a positive value, and it increased with increasing temperatures. Although high decolorization of DB-22 was achieved with the photo Fenton like process, low COD removal was observed at the studied conditions.

Acknowledgement

The author thank to Hitit University for their financial support of this project under contract of MUH19001.21.003.

489 **5. References**

- 490
- 491 1. A.S. Ejhieh, M. Khorsandi, *J Haz Mat.* **2010**, *176*, 629-637.
- **DOI:**10.1016/j.jhazmat.2009.11.077
- 493 2. M. Tekbas, H.C. Yatmaz, N. Bektas, Mic. Mes. Mat. 2008, 115, 594-602.
- **DOI:**10.1016/j.micromeso.2008.03.001
- 495 3. N. Demir, G. Gündüz, M. Dükkancı, Env. Sc. Poll. Res. 2015, 22, 3193-3201.
- 496 **DOI:**10.1007/s11356-014-2868-x
- 497 4. L.G. Devi, K.S.A. Raju, S.G. Kumar, K.E. Rajashekhar, J Taiw. Inst. Chem. Eng. 2011, 42, 341-
- 498 349.
- 499 **DOI:**10.1016/j.jtice.2010.05.010
- 5. F. Alakhras, E. Alhajri, R. Haounati, H. Ouachtak, A. Ait Addi, T.A. Saleh, Sur. Int. 2020, 20,
- 501 100611.
- **DOI:**10.1016/j.surfin.2020.100611
- 503 6. S.R. Pouran, A. Abdul Raman, W.M. Wan Daud, *J Cl. Prod.* **2014**, *64*, 24-35.
- **DOI:**10.1016/j.jclepro.2013.09.013
- 505 7. F. Sun, Q. Zeng, W. Tian, Y. Zhu, W. Jiang, *J Env. Chem. Eng.* **2019**, 7, 103011.
- **DOI:**10.1016/j.jece.2019.103011
- 507 8. J. Gao J, S. Ma, Z. Du, F. Cheng, P. Li, Wat. Sc. Tech. 2021, 83(2), 425-434.
- 508 **DOI:**10.2166/wst.2020.590
- 9. F.F. Brites-Nóbregaa, I.A. Lacerda, S.V. Santosa, C.C. Amorim, V.S. Santana, N.R.C Fernandes-
- 510 Machadoc, J.D. Ardisson, A.B. Henriques, M.D. Leão, *Cat. Tod.* **2015**, *240*, 168-175.
- **DOI:**10.1016/j.cattod.2014.06.036
- 512 10. G. Hu, J. Yang, X. Duan, R. Farnood, C. Yang, J. Yang, W. Liu, Q. Liu, Chem. Eng. J. 2021, 417,
- 513 129209.
- **DOI:**10.1016/j.cej.2021.129209
- 515 11. M.R. Abukhadra, A.S. Mohamed, *Silicon*, **2019**, *11*, 1635-1647.
- **DOI:**10.1007/s12633-018-9980-3
- 517 12. S. Benkhaya, S. M'rabet, A. El Harfi, *Heliyon*, **2020**, *6*(1), e03271.
- **DOI:**10.1016/j.heliyon.2020.e03271
- 13. N.T. Hien, L.H. Nguyen, H.T. Van, T.D. Nguyen, T.H.V. Nguyen, T.H.H. Chu, T.V. Nguyen,
- 520 V.T. Trinh, X.H. Vu, K.H.H. Aziz, Sep. Pur. Tech. 2020, 233, 115961.
- **DOI:**10.1016/j.seppur.2019.115961

- 14. J.R.S. Carvalho, F.M. Amaral, L. Florencio, M.T. Kato, T.P. Delforno, S. Gavazza, *Chem.* 2020,
- *242*, 125157.
- **DOI:**10.1016/j.chemosphere.2019.125157
- 525 15. R.K.M. Gomes, R.M.R. Santana, N.F.S. Moraes, S.G.S. Júnior, A.A. Lucena, L.E. Zaidan,
- 526 D.R.M. Elihimas, D.C. Napoleao, *Chem. Pap.* **2021**, *75*, 1993-2005.
- **DOI:** 10.1007/s11696-020-01451-4
- 528 16. O. Menezes, R. Brito, F. Hallwass, L. Florêncio, M.T. Kato, S. Gavazza, Chem Eng Res Des.
- **2019**, *146*, 369-378.
- **DOI:**10.1016/j.cherd.2019.04.020
- 531 17. H-Y. Shu, M-C. Chang, *J Haz Mat.* **2005**, *B121*, 127-133.
- **DOI:**10.1016/j.jhazmat.2005.01.020
- 533 18. A.B. Isaev, Z.M. Aliev, N.A. Adamadzieva, Russ. J App. Chem. 2012, 85(5), 765–769.
- 19. N.M. Mahmoodi, F. Najafi, S. Khorramfar, F. Amini, M. Arami, *J Haz. Mat.* **2011**, *198*, 87-94.
- **DOI:**10.1016/j.jhazmat.2011.10.018
- 536 20. M. Moosavifar, S.M. Heidari, L. Fathyunes, M. Ranjbar, Y. Wang, H. Arandiyan, *J Inorg. Org.*
- 537 *Poly. Mat.* **2020**, *30*, 1621-1628.
- **DOI:**10.1007/s10904-019-01277-y
- 539 21. K. Badvi, V. Javanbakht, *J Clean. Prod.* **2021**, 280, 124518.
- **DOI:**10.1016/j.jclepro.2020.124518
- 541 22. A.B. Rakhym, G.A. Seilkhanova, Y. Mastai, *Mic. Mes. Mat.* **2021**, *318*, 111020.
- **DOI:**10.1016/j.micromeso.2021.111020
- 543 23. T. Rashid, D. Iqbal, A. Hazafa, S. Hussain, F. Sher, F. Sher, J Env. Chem. Eng. 2020,
- *84(2)*, 104023.
- **DOI:**10.1016/j.jece.2020.104023
- 546 24. A. Abharya, A. Gholizadeh, *Cer. Int.* **2021**, *47*(9), 12010-12019.
- **DOI:**10.1016/j.ceramint.2021.01.044
- 548 25. S.R. Pouran, A. Bayrami, M.A. Shafeeyan, A.A. Abdul Raman, W.M.A. Wan Daud, Acta Chim.
- 549 *Slov.* **2018**, *65*(*1*), 166-171.
- **DOI:**10.17344/acsi.2017.3732
- 551 26. Ö. Dönmez, M. Dükkancı, G. Gündüz, J Env. Hea. Sci. Eng. 2020, 18, 835-851.
- **DOI:**10.1007/s40201-020-00507-7
- 553 27. P.P. Gan, S.F. Yau Li, Chem. Eng. J. 2013, 229, 351-363.
- **DOI:**10.1016/j.cej.2013.06.020

- 555 28. F. Ji, C. Li, J. Zhang, L. Deng, *J. Haz. Mat.* **2011**, *186*, 1979-1984.
- **DOI:**10.1016/j.jhazmat.2010.12.089
- 557 29. M. Karimi-Shamsabadi, M. Behpoura, A.K. Babaheidari, Z. Saberi, J Photoch. Photobio. A:
- 558 *Chem.* **2017**, *346*, 133-143.
- **DOI:**10.1016/j.jphotochem.2017.05.038
- 30. H. Sudrajat, S. Babel, *J Wat. Proc. Eng.* **2017**, *16*, 309-318.
- **DOI:**10.1016/j.jwpe.2016.11.006
- 31. D.S. Bhatkhande, V.G. Pangarkar, A.A Beenackers, *J Chem. Tech. Biotech.* **2002**, 77(1), 102-116.
- **DOI:**10.1002/jctb.532
- 32. R. Andrreozzi, V. Caprio, A. Insola, G. Longo, V. Tufano, J Chem. Tech. Biotech. 2000, 75, 131-
- 565 136.
- **DOI:**10.1002/(SICI)1097-4660(200002)75:2%3C131::AID-JCTB191%3E3.0.CO;2-F
- 33. S. Ahmed, Z. Ahmad, Env. Nan. Mon. Tech. 2020, 14, 100321.
- **DOI:**10.1016/j.enmm.2020.100321
- 569 34. D. Uzunoğlu, M. Ergüt, P. Karacabey, A. Özer, *Des. Wat. Treat.* **2019**, *172*, 96-105.
- **DOI:**10.5004/dwt.2019.24942
- 571 35. D. Çalık, D.I. Cifci, *J Env. Man.* **2022**, *304*, 114234.
- **DOI:**10.1016/j.jenvman.2021.114234
- 573 36. Z. Ghasemi, H. Younesi, A.A. Zinatizadeh, *J Taiw. Inst. Chem. Eng.* **2016**, *65*, 357-366.
- **DOI:**10.1016/j.jtice.2016.05.039
- 575 37. U.J. Ahile, R.A. Wuana, A.U. Itodo, R. Sha'Ato, R.F. Dantas, J Wat. Proc. Eng. 2020, 36,
- 576 101320.
- **DOI:**10.1016/j.jwpe.2020.101320
- 578 38. T.M. Jawad, M.R. AL-Lami, A.S. Hasan, J.A. Al-Hilfi, R.K. Mohammad, L.M. Ahmed, Egy. J
- 579 *Chem.* **2021**, *64*(9), 4857-4865.
- 580 **DOI:**10.21608/EJCHEM.2021.67501.3459
- 581 39. R. Saleh, A. Taufik, Sep. Pur. Tech. 2019, 210, 563-573.
- **DOI:**10.1016/j.seppur.2018.08.030
- 583 40. Y. Wang, J. Fang, J.C. Crittenden, C. Shen, *J Haz. Mat.* **2017**, *329*, 321-329.
- **DOI:**10.1016/j.jhazmat.2017.01.041